

Interactions of Calcineurin A, Calcineurin B, and Ca²⁺†

Bo Feng‡ and Paul M. Stemmer*·‡·§

Departments of Pediatrics, College of Medicine and Pharmaceutical Sciences, College of Pharmacy, University of Nebraska Medical Center, Omaha, Nebraska 68198-6055

Received March 2, 1999; Revised Manuscript Received July 8, 1999

ABSTRACT: Calcineurin B (CN-B) is the Ca²⁺-binding, regulatory subunit of the phosphatase calcineurin. Point mutations to Ca²⁺-binding sites in CN-B were generated to disable individual Ca²⁺-binding sites and evaluate contributions from each site to calcineurin heterodimer formation. Ca²⁺-binding properties of four CN-B mutants and wild-type CN-B were analyzed by flow dialysis confirming that each CN-B mutant binds three Ca²⁺ and that wild-type CN-B binds four Ca²⁺. Macroscopic dissociation constants indicate that N-terminal Ca²⁺-binding sites have lower affinity for Ca²⁺ than the C-terminal sites. Each CN-B mutant was coexpressed with the catalytic subunit of calcineurin, CN-A, to produce heterodimers with specific disruption of one Ca²⁺-binding site. Enzymes containing CN-B with a mutation in Ca²⁺-binding sites 1 or 2 have a lower ratio of CN-B to CN-A and a lower phosphatase activity than those containing wild-type CN-B or mutants in sites 3 or 4. Effects of heterodimer formation on Ca²⁺ binding were assessed by monitoring ⁴⁵Ca²⁺ exchange by flow dialysis. Enzymes containing wild-type CN-B and mutants in sites 1 and 2 exchange ⁴⁵Ca²⁺ slowly from two sites whereas mutants in sites 3 and 4 exchange ⁴⁵Ca²⁺ slowly from a single site. These data indicate that the Ca²⁺ bound to sites 1 and 2 is likely to vary with Ca²⁺ concentration and may act in dynamic modulation of enzyme function, whereas Ca²⁺-binding sites 3 and 4 are saturated at all times and that Ca²⁺ bound to these sites is structural.

Calcineurin is a Ca²⁺ and calmodulin-dependent serine/threonine phosphatase (1, 2) consisting of a catalytic subunit, calcineurin A (CN-A)¹ and a regulatory subunit, calcineurin B (CN-B). The two subunits are constitutively bound together and cannot be dissociated without denaturing the enzyme. While the CN-A catalytic domain shares sequence and structural homology with type-1 and type-2A phosphatases, a regulatory portion of CN-A, which does not have homology with other phosphatases, extends from the catalytic domain and folds back to cover the catalytic site with an autoinhibitory domain (3, 4). Calmodulin binding to the regulatory domain of CN-A produces release of the inhibition, presumably by promoting a more extended conformation for the regulatory region and preventing the autoinhibitory domain from folding back onto the catalytic site (4, 5). CN-B is irreversibly associated with CN-A at a site located at the beginning of the regulatory region and also interacts with residues in the amino terminal portion of CN-A (3, 6).

Though the details of how CN-B interacts with and regulates CN-A are not well defined, the essential role of CN-B in supporting calcineurin phosphatase activity and the

requirement of CN-B for Ca²⁺ are both well established (2, 7, 8). CN-B has four EF-hand Ca²⁺-binding sites which are important for the structural integrity of the enzyme, for activation of phosphatase activity and for recognition of inhibitory complexes (9, 10). The importance of Ca²⁺ in the interaction of CN-A with CN-B is suggested by data showing that when the subunits are expressed individually in an in vitro translation system, they require Ca²⁺ in order to bind together (11). The role of CN-B in enzyme activation has been demonstrated by showing that without CN-B the catalytic subunit has weak activity even in the presence of calmodulin and that the reconstituted calcineurin heterodimer has increased catalytic efficiency (increased K_{cat}/K_m) relative to isolated CN-A (12). The dependence of the enzyme on Ca²⁺ binding to CN-B was demonstrated using a calmodulin-independent fragment of calcineurin consisting of CN-B and the catalytic domain of CN-A plus a short extension of the regulatory domain to which CN-B binds (13). This calcineurin fragment, which cannot bind calmodulin, remains completely dependent on Ca²⁺ for activity (8). Using this calcineurin fragment, it was shown that CN-B has a role in regulating calcineurin activity by modulating K_m of the enzyme for its substrate (8). Binding of inhibitor complexes to calcineurin is also dependent on CN-B but not calmodulin (9, 14). The inhibitory complex binds to calcineurin only when Ca²⁺ is present, therefore, Ca²⁺ binding to CN-B is necessary for inhibitor complex binding. Although the crystal structures of CN-A, CN-B, and FK506/FKBP12 complexes have been solved (3, 6), how Ca²⁺ binding to CN-B acts to modulate inhibitor binding to calcineurin is not known.

Calcineurin phosphatase activity is regulated by two Ca²⁺-binding proteins: calmodulin and CN-B. Calmodulin is the

† This work was supported by Grant R29 GM51428 from the National Institute of General Medical Sciences.

* To whom correspondence should be addressed. Department of Pediatrics, 986055 Nebraska Medical Center, Omaha, NE 68198-6055. Phone: (402) 559-6461. Fax: (402) 559-5966. E-mail: pmstemme@unmc.edu.

‡ Department of Pharmaceutical Sciences, College of Pharmacy.

§ Department of Pediatrics, College of Medicine.

¹ Abbreviations: CN-B, calcineurin B; CN-A, calcineurin A; MLCK, myosin light chain kinase; ESR, electron spin resonance; DTT, dithiothreitol; SDS-PAGE, sodium dodecyl sulfate-polyacrylamide gel electrophoresis.

prototype for Ca²⁺-dependent regulator proteins and provides a standard to which CN-B can be compared. The clearest and easiest comparison of these two proteins is at the level of primary structure. CN-B has 35% sequence homology with calmodulin with the greatest degree of homology, 54%, in the four EF-hand Ca²⁺-binding sites. These Ca²⁺-binding domains constitute 76% of calmodulin and 67% of CN-B, indicating that Ca²⁺ binding is a critical function of each protein. The relationship between calmodulin, Ca²⁺, and target proteins is complex with the target modulating calmodulin interactions with Ca²⁺ as well as Ca²⁺ regulating the binding of calmodulin to targets (8, 15–17). It is not clear if a similar relationship exists for CN-B, Ca²⁺, and CN-A because the three participants are constitutively bound together. That is to say, isolated bovine brain calcineurin cannot be completely decalcified except under denaturing conditions. Initially, the proteolyzed form of calcineurin, which is devoid of the autoinhibitory and calmodulin-binding regions, was thought to be Ca²⁺ independent. Later studies showed that the proteolyzed enzyme does require Ca²⁺ and has a k_{act} of 0.06 μM for Ca²⁺ (8). Therefore, Ca²⁺-binding sites in CN-B responsible for enzyme activation can be decalcified and are clearly different from the structural sites which cannot be decalcified. The dichotomy of the Ca²⁺-binding sites suggests that there are two distinct and different parts of CN-B: one is structural and contains Ca²⁺ that is never removed, the other is regulatory with Ca²⁺ binding being transitory and important for enzyme activation or other properties of the phosphatase such as targeting.

It is evident that Ca²⁺ bound to CN-B is important for calcineurin structurally as well as serving to regulate the enzymes phosphatase activity or subcellular localization. To learn more about the roles of the individual Ca²⁺-binding sites of CN-B and the biochemical mechanism by which CN-B regulates calcineurin phosphatase, we have prepared a series of CN-B mutants, each of which is unable to bind Ca²⁺ at one site. For each of the four CN-B mutants a conserved glutamic acid residue at position 12 of one EF-hand Ca²⁺-binding loop was changed to lysine. The mutation in each Ca²⁺-binding site eliminated Ca²⁺ binding to one site in CN-B. Ca²⁺ binding to CN-B and the CN-B mutants was measured, and the role of individual Ca²⁺-binding sites in CN-B for protein association was evaluated.

MATERIALS AND METHODS

Materials. Restriction endonucleases, T4 DNA ligase, Taq polymerase and kanamycin were purchased from GIBCO BRL (Grand Island, New York) and Promega (Madison, WI). Prestained protein standards and DTT were from Bio-Rad (Richmond, CA). EDTA, ampicillin, aprotinin, and leupeptin were purchased from Sigma Chemical Co. (St. Louis, Missouri). The QuikChange site-directed mutagenesis kit was from Stratagene (La Jolla, CA). Phenyl-Sepharose, DEAE-Sepharose, and Sephadex G-75 media as well as the Mono-Q HR 5/5 column were purchased from Pharmacia LKB (Uppsala, Sweden). Nickel resins were from Invitrogen (Carlsbad, CA). ⁴⁵CaCl₂ was purchased from Dupont (Boston, MA). The pET28a vector was from Novagen (Madison, WI). PCR kits were from Perkin-Elmer Roche (Branchburg, NJ). BCA protein assay kit was purchased from Pierce (Rockford, IL). Standard solutions of CaCl₂ were obtained from Gallard Schlesinger. The 27-residue peptide, YWLP-

NFMDVFTWSLPLFVGEKVTMLVN, corresponding to amino acids Y₃₄₁–N₃₆₇ of CN-A which constitutes the core CN-B-binding domain of CN-A was synthesized by Dr. D. David Smith at Creighton University, Omaha, NE. The 19-residue peptide, KRRWKKNFIAVSAANRFKK-amide, corresponding to the calmodulin-binding domain of myosin light chain kinase (MLCK) (18) was a gift from Dr. Anthony Persechini at the University of Rochester Medical Center, Rochester, NY.

Expression and Purification of Human CN-B. A human CN-B expression plasmid designated pET28CN-B was produced by ligating PCR generated DNA fragments encoding CN-B into the *Nco*I–*Bam*HI sites of the pET28a expression vector. *Escherichia coli* BL21(DE3) were transformed with the ligation product and positive clones selected on kanamycin-LB plates. The sequence of the complete CN-B cDNA in pET28CN-B was verified by DNA sequencing at the UNMC core lab. Expression and purification of CN-B from pET28CN-B were accomplished as described (19). The homogeneity of isolated CN-B was greater than 95% as determined by SDS–PAGE with Coomassie staining. Protein concentrations were based on the CN-B extinction coefficients $\epsilon_{276\text{nm}}^{1\%} = 2.41$ (19) in 50 mM Tris-HCl, pH 7.5, 0.1 M NaCl, and 1 mM CaCl₂. All protein concentrations were verified using the BCA protein assay.

Site-Directed Mutagenesis. All mutations were introduced using the QuikChange site-directed mutagenesis kit. In each of the four CN-B mutants, the Glu at the 12 position of one EF-hand Ca²⁺-binding loop was replaced with a Lys. Plasmids containing the engineered CN-Bs were constructed from the pET28CN-B plasmid using the following primer pairs: site-1, E₄₂K, sense 5'-CTTTGAGTGTGGAAAAGTTCATGTCTCTGC-3', antisense 5'-GCAGAGACATGAAC-TTTTCCACTCAAAG-3'; site-2, E₇₄K, sense 5'-GAA-GTAGACTTTAAAAAATTCATTGAGGGCG-3', antisense 5'-CGCCCTCAATGAATTTTTTAAAGTCTACTTC-3'; site-3, E₁₁₁K, sense 5'-GGCTATATTTCCAATGGGAAACTCT-TCCAGG-3', antisense 5'-CCTGGAAGAGTTTCCCATTG-GAAATATAGCC-3'; site-4, E₁₅₂K, sense 5'-GGAAGAAT-ATCCTTTGAAAAATTCTGTGCTGTTGTAGG-3', antisense 5'-CCTACAACAGCACAGAATTTTTCAAAGGAT-ATTCTTCC-3'. All procedures for site-directed mutagenesis were conducted according to the manufacturers recommendation. The sequences of the CN-B mutants were verified by DNA sequencing. These plasmids are designated pET28M-1 through pET28M-4 for mutations in the first through fourth Ca²⁺-binding sites. The mutated proteins will be referred to as CN-B-E₄₂K, CN-B-E₇₄K, CN-B-E₁₁₁K, and CN-B-E₁₅₂K. *E. coli* B121(DE3) were transformed with pET28M-1 through pET28M-4 and the four mutant CN-Bs were expressed and purified using the same procedures as used for wild-type CN-B.

Expression of Calcineurin in *E. coli*. The plasmids pETCN- α (20) encoding CN-A and CN-B in a dicistronic construct and pBB131 (21) containing *Saccharomyces cerevisiae* myristoyl-coenzyme A: protein N-myristoyltransferase were kindly supplied by Drs. Liu and Gordon, respectively. Calcineurin was expressed in *E. coli* BL21-(pLysS)/pETCN α /pBB131 and purified as described (20). The CN-A subunit expressed in this system has an N-terminal polyhistidine tag, and the CN-B is myristoylated. Mutations

at individual Ca^{2+} -binding sites were introduced into CN-B in the pETCN- α construct using the same primers described earlier. The resultant plasmids are designated pETCN-M1 through pETCN-M4. The expression and purification of calcineurin mutants from pETCN-M1 through pETCN-M4 were done the same as for calcineurin expression and purification from pETCN- α (20). The enzyme containing wild-type CN-B is designated CN-WT and the four heterodimers containing CN-B with the single mutations E₄₂K, E₇₄K, E₁₁₁K, and E₁₅₂K are designated M₁, M₂, M₃, and M₄, respectively. The relative amounts of CN-B and CN-A in each isolated enzyme were estimated by laser densitometry (Molecular Dynamics) after electrophoresis of the proteins on SDS-PAGE.

Flow Dialysis. Ca^{2+} binding to CN-B and CN-B mutants was measured using the method of Colowick and Womack (22) with the dialysis chamber designed by Feldman (23) and the previously described modifications (8). The buffer used in these experiments consisted of 100 mM KCl, 1.0 mM MgCl_2 , and 10 mM HEPES, pH 7.5. When Ca^{2+} binding was examined in the presence of the CN-B-binding domain of CN-A, the peptide was present at 1.2 times the concentration of CN-B and the peptide was used without decalcification. Data were corrected for loss of Ca^{2+} and $^{45}\text{Ca}^{2+}$ from the flow well prior to calculating free and bound Ca^{2+} concentrations (8). Macroscopic dissociation constants K_1 , K_2 , K_3 , and K_4 (μM) were determined by fitting the data to 4 or 3 site Adair-Klotz equations with all parameters adjustable.

(A) Four site equation:

$$Y = N \frac{(x/K_1 + 2x^2/K_1K_2 + 3x^3/K_1K_2K_3 + 4x^4/K_1K_2K_3K_4)}{4(1 + x/K_1 + x^2/K_1K_2 + x^3/K_1K_2K_3 + x^4/K_1K_2K_3K_4)} + jx$$

(B) Three site equation:

$$Y = N \frac{(x/K_1 + 2x^2/K_1K_2 + 3x^3/K_1K_2K_3)}{3(1 + x/K_1 + x^2/K_1K_2 + x^3/K_1K_2K_3)} + jx$$

Y is the number of moles of Ca^{2+} bound per moles of CN-B, N is the ratio of actual to measured protein concentration, x is free Ca^{2+} concentration, K_1 – K_4 are macroscopic dissociation constants, and j is a factor to account for nonspecific binding. Data were fit to eqs A and B using the Prism (GraphPad, Inc.) software package.

For examination of rates of Ca^{2+} exchange between protein bound $^{45}\text{Ca}^{2+}$ and Ca^{2+} free in solution, bovine brain calcineurin was incubated with 10-fold molar excess of $^{45}\text{Ca}^{2+}$ for 1 h at 22 °C then separated from unbound $^{45}\text{Ca}^{2+}$ by gel filtration and added to the flow well at a final concentration of 5 μM . For examination of rates of Ca^{2+} exchange between *E. coli* expressed enzymes and Ca^{2+} free in solution, the proteins were equilibrated with $^{45}\text{Ca}^{2+}$ at 22 °C, then unbound $^{45}\text{Ca}^{2+}$ was removed by passing the protein solution over a 0.8 mL bed of chelex resin at 4 °C. Calmodulin was decalcified with chelex, and 1.2 mole equivalents of the calmodulin-binding domain peptide from MLCK and 0.8 mol of $^{45}\text{Ca}^{2+}$ /mol or calmodulin were added to the flow well. Exchange of bound $^{45}\text{Ca}^{2+}$ was initiated by addition of 2 mM CaCl_2 .

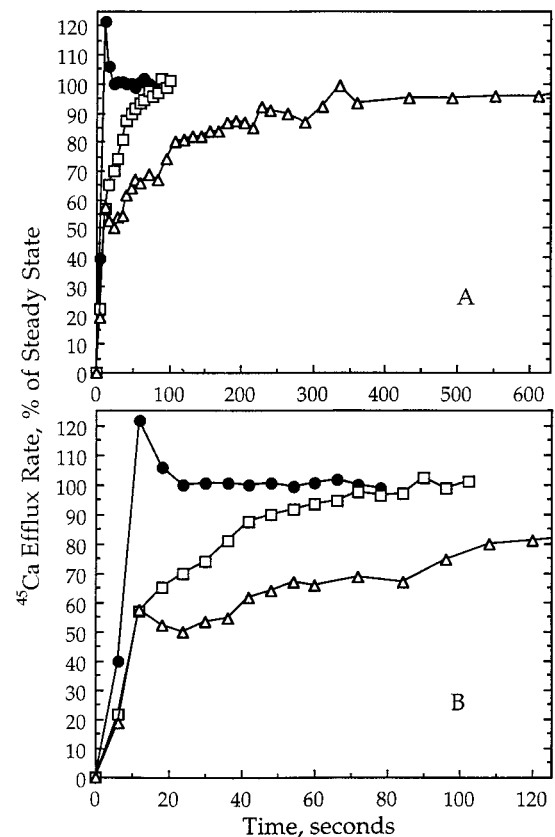


FIGURE 1: $^{45}\text{Ca}^{2+}$ efflux from flow dialysis chamber upon addition of 2 mM CaCl_2 to the chamber containing $^{45}\text{Ca}^{2+}$ bound to: calmodulin plus the peptide corresponding to the calmodulin binding domain of MLCK (\square), bovine brain calcineurin (Δ). Filled circles (\bullet), represent efflux when tracer $^{45}\text{Ca}^{2+}$ was added to the flow well simultaneously with the 2 mM CaCl_2 . Panel B is an expanded view of the data shown in the first part of panel A.

Phosphatase Activity. Calcineurin phosphatase activity was assayed as previously described (24). The enzymes were incubated at 30 °C in buffer containing 40 mM Tris-HCl, pH 7.5, 100 mM KCl, 6 mM MgCl_2 , 0.1 mM dithiothreitol, 0.1 mg/mL bovine serum albumin, 100 μM CaCl_2 , 50 nM enzyme, and 100 nM calmodulin. Reactions were started by addition of phosphorylated peptide substrate DLDVPIGR-FDRRVSAAE (25) to a final concentration of 1 μM and stopped after 30 min.

RESULTS

$^{45}\text{Ca}^{2+}$ Exchange from Calcineurin. Because bovine brain calcineurin cannot be decalcified without denaturing the protein, the affinity of CN-B Ca^{2+} -binding sites for Ca^{2+} has not been determined using standard methods. To make an estimate of the affinity of Ca^{2+} -binding sites in intact calcineurin for Ca^{2+} , the dissociation rate constant for $^{45}\text{Ca}^{2+}$ pre-equilibrated with bovine brain calcineurin was estimated by flow dialysis. The rate of $^{45}\text{Ca}^{2+}$ exchange from calmodulin plus the calmodulin-binding domain peptide from MLCK was determined in parallel to provide a reference to established methods for estimating k_{-1} for Ca^{2+} release from EF-hand Ca^{2+} -binding proteins (26). Figure 1A shows the time course to steady state for $^{45}\text{Ca}^{2+}$ efflux from the flow dialysis chamber in the absence of protein, in the presence of calmodulin, plus the calmodulin-binding domain of

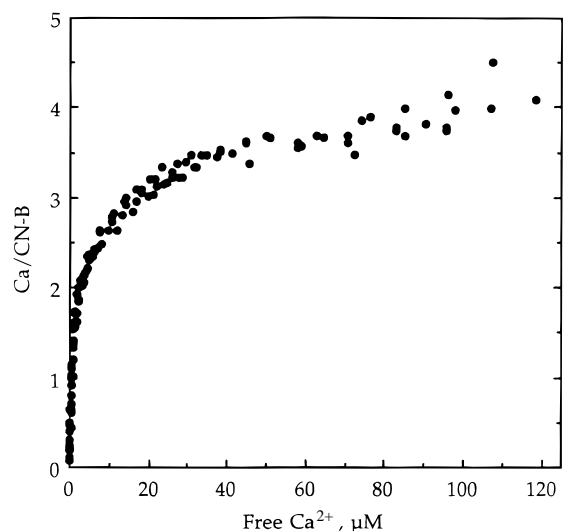


FIGURE 2: Flow dialysis determination of Ca^{2+} binding to *E. coli* expressed wild-type CN-B. Pooled data from five independent runs, CN-B concentration was 10 μM .

MLCK, or in the presence of bovine brain calcineurin. The record in the absence of protein was obtained by adding 2.0 mM CaCl_2 with $^{45}\text{Ca}^{2+}$ as a tracer to the chamber at time zero and reflects the response time of the system. The early time points from Figure 1A are replotted in Figure 1B on an expanded scale to show the initial surge of $^{45}\text{Ca}^{2+}$ efflux that occurs with addition of 2.0 mM CaCl_2 to the chamber. This transient surge in $^{45}\text{Ca}^{2+}$ efflux dissipates quickly and $^{45}\text{Ca}^{2+}$ efflux rate reaches steady state 24 s after introducing the Ca^{2+} . As shown in Figure 1A, $^{45}\text{Ca}^{2+}$ bound to calmodulin plus peptide requires more than 60 s to fully exchange with free Ca^{2+} in the dialysis chamber and that bound to calcineurin requires greater than 300 s. The time courses for $^{45}\text{Ca}^{2+}$ efflux from the chamber containing calmodulin plus peptide and that containing calcineurin are indistinguishable over the first 12 s (Figure 1B). This initial surge in $^{45}\text{Ca}^{2+}$ efflux is analogous to the surge observed for the protein free chamber and is attributed to a rapid exchange of $^{45}\text{Ca}^{2+}$ from relatively low-affinity sites on the proteins. The divergence of the efflux patterns after the initial surge reflects a difference in the rate of Ca^{2+} exchange from the two proteins. Ca^{2+} exchange from calcineurin is much slower than from calmodulin plus peptide. For each protein, the data after the initial surge were fit to a monoexponential decay model. The dissociation rate constants calculated for Ca^{2+} release from calmodulin plus peptide and from calcineurin are 0.048 ± 0.002 and $0.0098 \pm 0.0008 \text{ s}^{-1}$ (mean \pm SEM), respectively.

Ca^{2+} Binding to CN-B. Flow dialysis was used to measure Ca^{2+} binding to *E. coli* expressed CN-B, and binding data were fit to the Adair–Klotz equation (8, 27). Because the CN-B sequence indicates that the protein has four EF-hand Ca^{2+} -binding sites and four Ca^{2+} are identified in crystal structures of calcineurin (3, 6), a four binding site model (8) was used to analyze the Ca^{2+} -binding data for CN-B. Ca^{2+} binding to wild-type CN-B (Figure 2), reached an apparent saturation at four Ca^{2+} per CN-B. The macroscopic dissociation constants for Ca^{2+} binding to CN-B are shown in Table 1.

Site-Directed Mutagenesis of CN-B. The four EF-hand Ca^{2+} -binding sites in CN-B are numbered I–IV from the N-terminus. Glu12 is the most conserved amino acid in the

EF-hand Ca^{2+} -binding loops and studies of calmodulin have shown that mutation of Glu12 to Lys12 is likely to abolish Ca^{2+} binding (28). Sequences of the Ca^{2+} -binding loops of the four CN-B mutants are shown in Figure 3. To confirm that each CN-B mutant had lost one Ca^{2+} -binding site, flow dialysis was used to examine the Ca^{2+} -binding properties of those proteins. Binding of Ca^{2+} to each of the CN-B mutants is shown in Figure 4. Binding data for each of the mutants fit well using a three-site model but was unable to fit a four-site model. Calculated macroscopic dissociation constants for the proteins are shown in Table 1. In comparing the affinities of the four CN-B mutants for Ca^{2+} , it is clear that both loop 1 and loop 2 CN-B mutants produce Ca^{2+} binding data that is best fit using a model with two relatively high affinity sites and one lower affinity site whereas data from loop 3 and loop 4 CN-B mutants fit a model with one relatively high affinity site and two lower affinity sites.

Effects of CN-B-Binding Domain Peptide on the Ca^{2+} -Binding Affinity of CN-B. The affinity of CN-B for Ca^{2+} as an independent protein (Table 1) is much lower than it is for CN-B as part of intact bovine brain calcineurin (Figure 1). To determine if a peptide corresponding to the CN-B-binding domain of CN-A would increase the affinity of CN-B for Ca^{2+} , flow dialysis experiments were performed with CN-B in the presence of this peptide. Crystal structures of intact calcineurin have shown that the major contacts between CN-A and CN-B are within the 27 amino acid long stretch of CN-A between Y₃₄₁ and N₃₆₇ (3, 6). This CN-A peptide is likely to constitute the core CN-B-binding domain but does not eliminate the possibility that other residues in CN-A contribute to stabilizing the CN-B/CN-A interaction. Peptide concentration was estimated using an $\epsilon_{280\text{nm}}^{\text{M}}$ of 12 660 (29), and the ratio of protein to peptide during the binding experiment was set at 1:1.2. Figure 5 shows Ca^{2+} binding to CN-B in the presence and absence of the CN-A peptide Y₃₄₁–N₃₆₇. It is clear that the tested peptide did not increase the affinity of CN-B for Ca^{2+} and fitting of the data produced binding constants which were not significantly different from those found for CN-B itself.

Calcineurin Heterodimers With Mutant CN-B. Calcineurin heterodimers containing wild-type CN-B or CN-Bs with a single mutation were expressed as described (20) and the myristoylation of CN-B subunits was confirmed by their increased mobility on SDS–PAGE. The enzyme containing wild-type CN-B is designated CN-WT and the four heterodimers containing CN-B with the single mutations E₄₂K, E₇₄K, E₁₁₁K, and E₁₅₂K are designated M₁, M₂, M₃, and M₄, respectively. CN-WT and M₁–M₄ were expressed and partially purified using a single step affinity chromatography on Ni²⁺ columns. These proteins were examined by SDS–PAGE to determine effects of the mutations on CN-B mobility during electrophoresis. All the CN-Bs have similar mobility on SDS–PAGE in the absence of Ca^{2+} (Figure 6). In the presence of Ca^{2+} , the CN-Bs from M₃ and M₄ migrate slower than wild-type CN-B or CN-Bs from the M₁ or M₂ enzymes. This decrease in the magnitude of the Ca^{2+} -induced mobility shift is consistent with Ca^{2+} -binding sites 3 and 4 having a higher affinity for Ca^{2+} and indicates that Ca^{2+} -dependent changes in mobility of CN-B on SDS–PAGE are due to Ca^{2+} binding to sites 3 and 4.

Table 1: Ca²⁺ Binding to CN-B and CN-B Mutants^a

macroscopic constant (μM)	wild-type CN-B	loop 1 CN-B-E ₄₂ K	loop 2 CN-B-E ₇₄ K	loop 3 CN-B-E ₁₁₁ K	loop 4 CN-B-E ₁₅₂ K
K_1	0.36 ± 0.13	0.17 ± 0.03	0.14 ± 0.01	2.34 ± 0.21	1.71 ± 0.43
K_2	0.94 ± 0.16	1.82 ± 0.01	0.63 ± 0.16	7.78 ± 2.52	3.16 ± 0.43
K_3	11.2 ± 2.4	50.6 ± 6.6	14.5 ± 1.1	36.2 ± 8.2	32.5 ± 13.8
K_4	36.5 ± 10.7				
n	4	2	2	2	3

^a Macroscopic dissociation constants for Ca²⁺ binding to wild-type CN-B and the four single site mutants of CN-B. Ca²⁺ binding was determined for each protein using flow dialysis and the data fit to the Adair-Klotz equation. Individual experiments were analyzed independently. Values represent the mean ± standard deviation when $n > 2$ and the mean ± range for $n=2$.

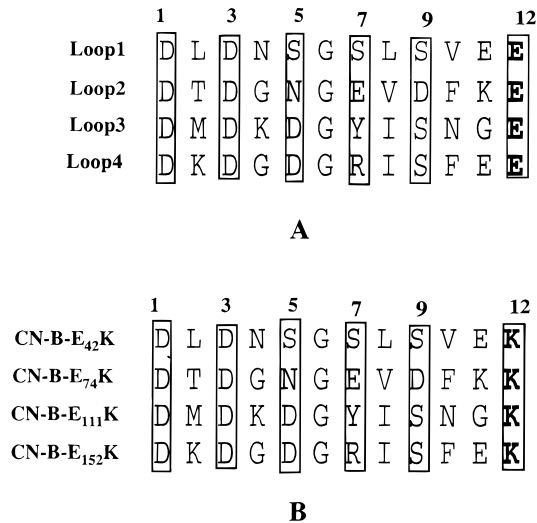


FIGURE 3: Comparison of the amino acid sequences of the four Ca²⁺-binding loops in human CN-B and in the four mutants of CN-B. Numbers placed over boxed residues indicate those amino acids are coordinating sites for Ca²⁺.

Quantitative densitometry was used to estimate the ratio of CN-B to CN-A in CN-WT as well as M₁–M₄ (Table 2). The partially purified enzymes were separated on SDS-PAGE as shown in Figure 6. The relative density for bands corresponding to CN-B and CN-A for each enzyme is shown in Table 2. Calcineurin B has a molecular weight of 19 167 in comparison to 58 555 for calcineurin A. The mass ratio of CN-B:CN-A is, therefore, 0.33, and a 1:1 complex of the two proteins is expected to produce a similar density ratio after SDS-PAGE and Coomassie staining. CN-WT, M₃, and M₄ each have the same ratio of CN-B to CN-A, whereas the M₁ and M₂ enzymes have a decrease in CN-B associated with the CN-A (Table 2).

Phosphatase Activity. Calcineurin phosphatase activity of the *E. coli* expressed enzymes was assayed using a phosphopeptide substrate. Figure 7 shows activity of each enzyme in the absence and presence of excess calmodulin. CN-WT, M₃, and M₄ have similar activities whereas M₁ and M₂ have substantially reduced phosphatase activity. All five enzymes have an increase in phosphatase activity in the presence of calmodulin. Because these assays were conducted with saturating Ca²⁺, it is not known if any of the enzymes have an altered sensitivity to Ca²⁺.

Ca²⁺ Binding to Calcineurin Heterodimers. Because the isolated CN-B does not bind Ca²⁺ with the same high affinity seen in bovine brain calcineurin and because the core CN-B-binding domain from CN-A does not increase the affinity of isolated CN-B for Ca²⁺, some aspect of the formation of the intact heterodimeric enzyme must confer a structural role

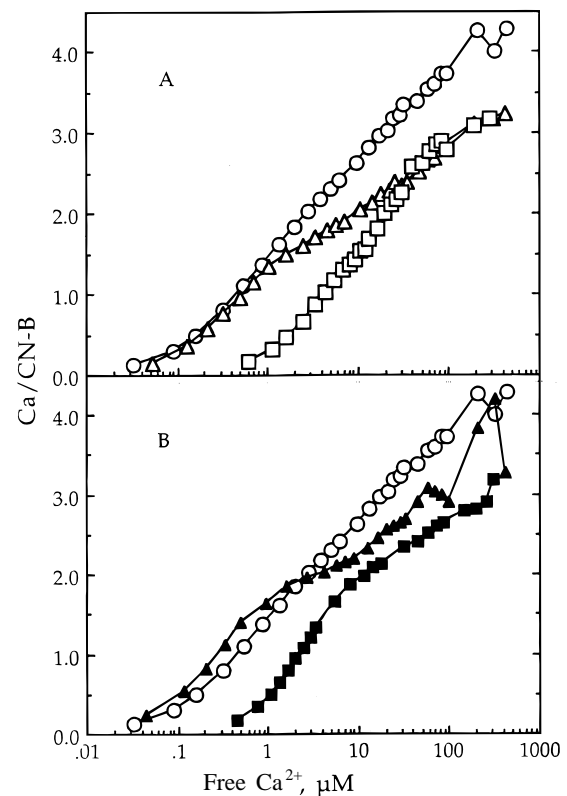


FIGURE 4: Flow dialysis determination of Ca²⁺ binding to *E. coli* expressed wild-type CN-B (○), and mutants of CN-B with inactivated EF-hand Ca²⁺-binding sites 1 (△), or 3 (□) (panel A), and 2 (▲), or 4 (■) (panel B). Representative data from two or three independent runs for each mutant and from five runs of wild-type CN-B. Protein concentration was 10 μM .

to two of the Ca²⁺-binding sites in CN-B, which makes exchange of Ca²⁺ from those sites extremely slow. To determine if enzymes M₁–M₄ contained the structural Ca²⁺-binding sites observed in bovine brain calcineurin, the rate of ⁴⁵Ca²⁺ exchange from each of the enzymes was determined. Time courses for ⁴⁵Ca²⁺ exchange from enzyme to solution are shown in Figure 8. As shown in Figure 1, the flow dialysis technique is not able to generate usable measurements for the first part of the exchange. Therefore, data from 27 to 500 s were used to calculate ⁴⁵Ca²⁺ exchange rates for expressed enzymes. Data for the increase in ⁴⁵Ca²⁺ efflux rate from the chamber were fit to single and double exponential decay models with the results presented in Table 3. The values in Table 3 for the fraction of ⁴⁵Ca²⁺ exchanged from each site represent the ⁴⁵Ca²⁺ exchanging from a site in the measurable time period after the initial 27 s. ⁴⁵Ca²⁺ exchanging from rapidly equilibrating sites and from the slowly equilibrating sites during the initial 27 s account for

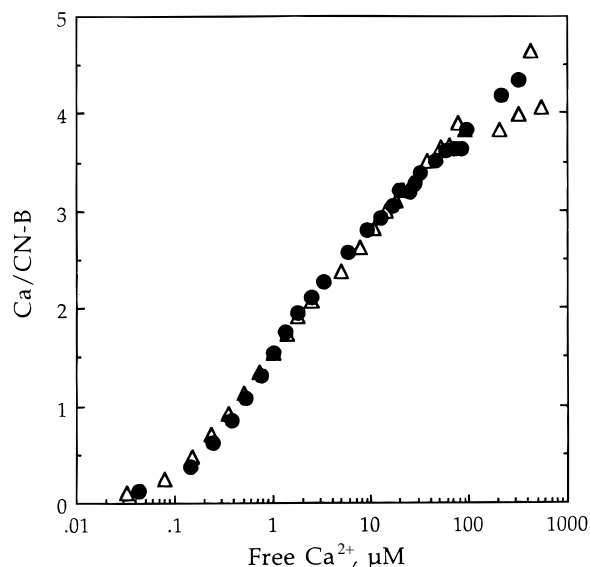


FIGURE 5: Flow dialysis determination of Ca^{2+} binding to *E. coli* expressed wild-type CN-B in the presence (●) and absence (△) of a peptide corresponding to the core CN-B-binding domain of CN-A.

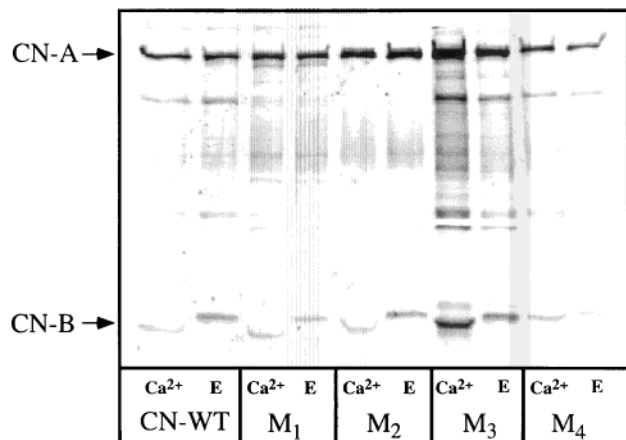


FIGURE 6: Ca^{2+} -dependent mobility shift on SDS-PAGE for wild-type CN-B and four mutants of CN-B. Enzymes were isolated by a single step purification on Ni^{2+} resins then sampled for electrophoresis. Samples contained either 1 mM CaCl_2 (Ca^{2+}) or 1 mM EGTA (E).

Table 2: CN-B Associated with CN-A^a

enzyme	CN-B/CN-A
WT-CN	0.24 ± 0.01
M ₁	0.14 ± 0.02
M ₂	0.16 ± 0.03
M ₃	0.24 ± 0.02
M ₄	0.27 ± 0.01

^a Relative density of CN-B band to CN-A band as determined by laser densitometry of SDS-PAGE gels on which the indicated *E. coli* expressed enzymes were run. Each enzyme was purified and analyzed four independent times. Mean ± standard deviation are presented.

the remaining $^{45}\text{Ca}^{2+}$ bound at the initiation of exchange. CN-WT, M₁, and M₂ have indistinguishable dissociation rate constants for exchange of $^{45}\text{Ca}^{2+}$ and the data fit best to a two exponential model. In comparison to CN-WT, M₁, and M₂ have a larger slowly exchanging component of $^{45}\text{Ca}^{2+}$. This is attributed to loss of a rapidly exchanging site by mutation of either site 1 or site 2. Data for exchange of $^{45}\text{Ca}^{2+}$ from M₃ and M₄ could not be fit to a two exponential

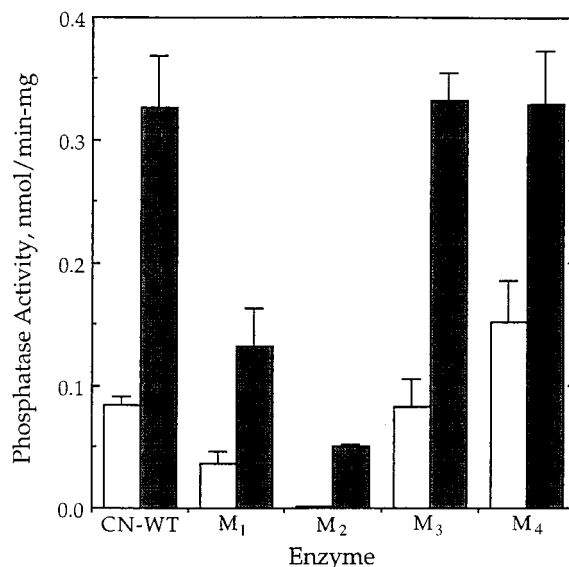


FIGURE 7: Phosphatase activity of CN-WT and four enzymes with point mutations in the Ca^{2+} binding loops of calcineurin B. Open bars represent activity in the absence of calmodulin and filled bars represent activity in the presence of calmodulin. Ca^{2+} was 100 μM under both conditions. Values are mean ± SEM, $n = 3$.

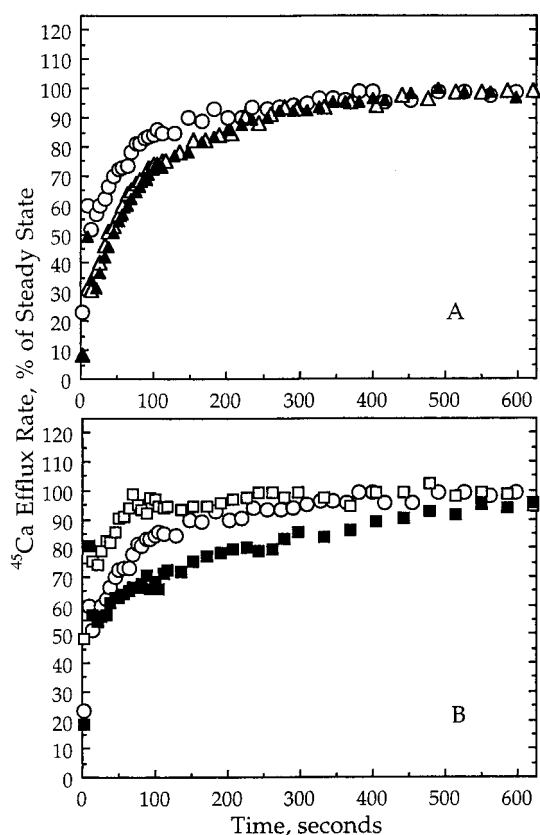


FIGURE 8: Flow dialysis determination of the rate of $^{45}\text{Ca}^{2+}$ efflux from the flow dialysis chamber upon addition of 2 mM CaCl_2 to the chamber containing $^{45}\text{Ca}^{2+}$ bound to: CN-WT (O), and M₁ (△), or M₂ (▲) (panel A), and M₃ (□), or M₄ (■) (panel B). Representative data from two independent runs for each enzyme.

process model but does fit well to a single-exponential process model. $^{45}\text{Ca}^{2+}$ bound to the slowly exchanging Ca^{2+} -binding site retained in M₃ exchanges more rapidly than that bound to the slowly exchanging site in M₄. On the basis of the rate constants shown in Table 3, sites 3 and 4 in calcineurin B are designated as structural sites.

Table 3: Rates for $^{45}\text{Ca}^{2+}$ Exchange from Calcineurin^a

enzyme	best fit model		fraction (% of total)	k_{-1} (s^{-1})
WT-CN	2 site	i	19.5	0.0044 (0.0022)
		ii	19.1	0.0313 (0.0093)
M ₁	2 site	i	36.1	0.0057 (0.0005)
		ii	18.2	0.0291 (0.0040)
M ₂	2 site	i	40.3	0.0056 (0.0006)
		ii	20.0	0.0324 (0.0053)
M ₃	1 site		15.8	0.0369 (0.0080)
M ₄	1 site		36.9	0.0039 (0.0006)

^a Exchange of $^{45}\text{Ca}^{2+}$ from *E. coli* expressed calcineurins was initiated by addition of 2 mM CaCl_2 and monitored by flow dialysis. Data from 27 to 500 s after the initiation of exchange were analyzed for one and two component exponential decay and the best fit presented. The 27 s time point was set as time zero to avoid the $^{45}\text{Ca}^{2+}$ surge at initiation of exchange. The fraction of total $^{45}\text{Ca}^{2+}$ assigned to each site represents the fraction of $^{45}\text{Ca}^{2+}$ bound to the protein at initiation of exchange which dissociates from the protein after the initial 27 s. Values are the best fit of data from a representative experiment with SEM for k_{-1} in parentheses. Each protein was examined two times.

DISCUSSION

Calcineurin is known to have such high affinity for Ca^{2+} that it cannot be decalcified using nondenaturing methods (8). At the same time, Ca^{2+} in the micromolar range and above activates calcineurin in vitro (8) and supports inhibitor binding (9, 10). The large difference in affinity for Ca^{2+} binding to different sites in calcineurin indicates that there are two distinct functions of Ca^{2+} binding to CN-B, structural, and activation or targeting. Direct measurement of the kinetics of $^{45}\text{Ca}^{2+}$ exchange from bovine brain calcineurin and of Ca^{2+} binding to CN-B and mutants of CN-B which have lost one Ca^{2+} -binding site have allowed us to estimate the affinity of structural Ca^{2+} -binding sites in calcineurin and assign the structural and activation functionalities to the carboxyl and amino halves of CN-B, respectively.

Flow dialysis is a very slow process relative to detection of fluorescence, so only slow exchange processes can be studied using this technique. The k_{-1} for Ca^{2+} dissociation from the calmodulin-MLCK peptide complex into a chelator solution which effectively decalcifies the complex has been measured to be 0.15 s^{-1} (26). The value of k_{-1} for $^{45}\text{Ca}^{2+}$ exchange from this same complex determined by flow dialysis, as shown in Figure 1, is 0.048 s^{-1} . One important difference between these systems is that the dissociation observed by fluorescence occurs into a chelator solution, and therefore, it occurs from complexes having 4, 3, 2, and 1 Ca^{2+} bound. Ca^{2+} binding to the calmodulin-peptide complex is highly cooperative, and loss of any one Ca^{2+} is predicted to increase the dissociation rate constant for the Ca^{2+} ions remaining bound. In the flow dialysis system, $^{45}\text{Ca}^{2+}$ is exchanged between a Ca^{2+} saturated complex and a large excess of free Ca^{2+} in solution. An association rate constant, k_1 , equal to $2.3 \times 10^6 \text{ M}^{-1} \text{ s}^{-1}$ for Ca^{2+} binding to calmodulin plus the MLCK peptide, was calculated from the published dissociation rate constant of 0.15 s^{-1} (26), and the measured K_D of 65 nM for Ca^{2+} binding to the same calmodulin plus peptide mixture (Stemmer, unpublished results). The association rate constant for Ca^{2+} binding to the calmodulin peptide complex indicates that Ca^{2+} binding from a solution containing 1 mM Ca^{2+} is fast relative to Ca^{2+} dissociation from the calmodulin-peptide- Ca^{2+}_3 complex.

Therefore, all exchange will occur from the fully saturated calmodulin-peptide- Ca^{2+}_4 complex. Under these conditions, cooperativity in Ca^{2+} binding will be maintained and the measured k_{-1} is expected to be small relative to the k_{-1} for Ca^{2+} dissociation into a chelator solution. This is precisely what we observe in our experiments, and this finding indicates that flow dialysis is capable of measuring Ca^{2+} exchange rate constants less than k_{-1} of 0.05 s^{-1} .

Exchange of $^{45}\text{Ca}^{2+}$ from bovine brain calcineurin occurs in two distinct phases. The very rapid increase in $^{45}\text{Ca}^{2+}$ efflux rate from the dialysis chamber upon addition of excess CaCl_2 accounts for about half of bound $^{45}\text{Ca}^{2+}$. This component of bound Ca^{2+} accounts for two of the four Ca^{2+} -binding sites in CN-B, is in rapid equilibrium with the solution, and is likely to represent Ca^{2+} bound to activating sites. The remaining two sites have a very slow exchange of Ca^{2+} with the solution. Using the exchange rate determined by flow dialysis, 0.0098 s^{-1} , as an estimate of k_{-1} and an association rate constant estimated from the k_1 of $2.3 \times 10^6 \text{ M}^{-1} \text{ s}^{-1}$ for Ca^{2+} binding to calmodulin plus the MLCK peptide, the K_D of high-affinity-binding sites in intact calcineurin for Ca^{2+} is calculated to be $4.2 \times 10^{-9} \text{ M}$. This estimate for the affinity of these two sites is substantially higher than the measured affinities of Ca^{2+} -binding sites in isolated CN-B for Ca^{2+} , which range from 0.36×10^{-6} to $36.5 \times 10^{-6} \text{ M}$. This high affinity indicates that CN-A must have an action to increase the affinity of CN-B for Ca^{2+} and that two sites in CN-B will be saturated with Ca^{2+} at all times in living cells. These high affinity sites are, therefore, considered to be structural sites.

The slow exchange rate for Ca^{2+} bound to bovine brain calcineurin and the estimated high affinity of the structural Ca^{2+} -binding sites in that enzyme contrast sharply with the measured affinity of isolated CN-B for Ca^{2+} . Formation of the calcineurin heterodimer in some way confers a structural role on two of the Ca^{2+} -binding sites in CN-B and upon the Ca^{2+} bound to those sites. As shown by direct measurement of $^{45}\text{Ca}^{2+}$ binding, the core CN-B-binding domain of CN-A is not able to increase the affinity of CN-B for Ca^{2+} at any of the four sites (Figure 5). This is unexpected due to the high affinity of the intact enzyme for Ca^{2+} and is in contrast to the increase in affinity for Ca^{2+} that calmodulin shows in the presence of calmodulin binding domain peptides (8, 15–17). The inability of the core CN-B-binding domain from CN-A to affect the affinity of CN-B for Ca^{2+} indicates that additional domain(s) within the intact CN-A molecule must contribute to stabilizing the intact enzyme.

Comparing the macroscopic binding constants for wild-type CN-B and the four CN-B mutants provides some insight as to the identity and independence of the four sites. From the values shown in Table 1, it is apparent that the two sites in the amino terminal half of CN-B are the lower affinity sites with dissociation constants in the 10–50 μM range. In contrast, sites 3 and 4, in the carboxyl half of isolated CN-B, have submicromolar affinity for Ca^{2+} . The different mobility of CN-B and single site CN-B mutants on SDS-PAGE in the presence of Ca^{2+} supports the assignment of sites 3 and 4 as higher affinity sites in the isolated CN-B. Reduction in magnitude of the mobility shift for site 3 and site 4 mutants is most likely due to a decreased ability of those proteins to bind Ca^{2+} under conditions of the electrophoresis. Positive cooperativity in binding is common among

EF-hand Ca^{2+} -binding proteins such as calmodulin and troponin C. In these proteins, pairs of EF-hand Ca^{2+} -binding sites rather than single EF-hand sites are the functional units (30). The crystal structure of CN shows that CN-B consists of two globular Ca^{2+} -binding regions flanked by a long C-terminal β -strand. Each half of CN-B contains two Ca^{2+} -binding EF-hand motifs which may function as a pair. The decrease in affinity for the first Ca^{2+} bound to site 3 and site 4 mutants of CN-B suggests that these two sites do function as a pair and have positive cooperativity in binding Ca^{2+} .

Because Ca^{2+} -binding sites important for activation can be depleted of Ca^{2+} without any effect on heterodimer stability, loss of the ability to bind Ca^{2+} at the activation sites is not expected to affect heterodimer formation. As shown in Table 2, the ratio of CN-B:CN-A is decreased by the mutations which block Ca^{2+} binding to sites 1 or 2 of CN-B but is unaffected by mutations to sites 3 or 4. These data are consistent with the amino terminal half of CN-B contributing to formation of the heterodimer. However, because sites 3 and 4 are clearly the slow exchange Ca^{2+} binding sites, it is likely that the mutations in sites 1 and 2 decrease heterodimer formation by changing the conformation of CN-B in a manner unrelated to Ca^{2+} binding. It is not known if such a conformational change would also inhibit Ca^{2+} -dependent enzyme activation and account for the low phosphatase activity of enzymes containing CN-B with site 1 and site 2 mutations. An additional possibility is that the decrease in the CN-B:CN-A ratio in M_1 and M_2 contributes to the low phosphatase activity seen with these enzymes.

The equilibrium Ca^{2+} binding data in Table 1 and the SDS-PAGE mobility shift data in Figure 6 show that sites 3 and 4 of isolated CN-B have higher affinity for Ca^{2+} than sites 1 and 2. Although this is consistent with sites 3 and 4 in the heterodimer being structural sites, the structural sites are a property only of the heterodimer and comparison of data from the enzyme with data from the isolated CN-B subunit is not appropriate. Expression of heterodimers with single site CN-B mutants has allowed unambiguous assignment of the structural sites by determination of $^{45}\text{Ca}^{2+}$ exchange rates for the mutants. The M_1 and M_2 enzymes retain the slow dissociating component of $^{45}\text{Ca}^{2+}$, and the increase in the fraction of $^{45}\text{Ca}^{2+}$ that dissociates most slowly in these enzymes indicates that a rapidly dissociating Ca^{2+} -binding site is lost. Exchange of $^{45}\text{Ca}^{2+}$ from the M_3 and M_4 enzymes could not be fit to a two exponential process indicating that each of these enzymes had lost one of the slow dissociating sites. Exchange of $^{45}\text{Ca}^{2+}$ is more rapid from M_3 than from M_4 , indicating that these sites are not equivalent and that the effects of heterodimer formation are greatest on Ca^{2+} -binding site 3.

The Ca^{2+} -binding studies presented here are consistent with intact calcineurin containing two high-affinity structural sites and two lower affinity activation sites as described for proteolyzed bovine brain calcineurin (8). This interpretation is also supported by the X-band electron spin resonance spectroscopy (ESR) studies which describe Mn^{2+} binding to CN-B (31). In those studies, Wei et al. (31) used X-band ESR to investigate the binding of Mn^{2+} to CN-A, CN-B, and to the intact enzyme. They found that intact bovine brain calcineurin bound only 2 mol of Mn^{2+} /mol of enzyme, whereas the individual CN-A and CN-B subunits bound 2

and 4 mol of Mn^{2+} /mol, respectively. The inaccessibility of four Mn^{2+} -binding sites in the heterodimer, which are available when the subunits are separated, indicates that formation of the calcineurin heterodimer qualitatively changes at least two Ca^{2+} -binding sites in CN-B. The slow exchange of two Ca^{2+} from CN-B in the intact enzyme shown in Figures 1 and 8 extends the previous work, showing that the proteolyzed, calmodulin-independent calcineurin contains two high-affinity Ca^{2+} sites ($K_D < 0.07\mu\text{M}$) and one or two low-affinity sites ($K_D > 0.07\mu\text{M}$) (8) by supporting a structural role for two Ca^{2+} in the calcineurin heterodimer.

Calcineurin is unique in being regulated by two different Ca^{2+} -binding proteins, calmodulin and CN-B. The role of CN-B and of the Ca^{2+} -binding sites in CN-B is still an open question. Work presented here demonstrates the presence of two structural Ca^{2+} -binding sites in CN-B and provides evidence that those sites are in the carboxyl half of the protein. The residues in CN-A that contribute to stabilizing Ca^{2+} binding to CN-B and contribute to formation of a structural unit remain to be identified. Two possibilities are the amino terminal portion of CN-A and the remainder of the regulatory domain that extends from the core CN-B-binding domain. Conformational changes which occur upon Ca^{2+} binding to the activation sites in the amino half of CN-B are expected to produce functional changes in the enzyme. It is likely that these effects are directly on the catalytic domain of CN-A as the proteolyzed enzyme which does not contain the remainder of the regulatory domain retains the requirement for Ca^{2+} for activation (8).

ACKNOWLEDGMENT

We thank Drs. Jun Liu and Jeffrey I. Gordon for providing plasmids for expression of calcineurin and myristoyl transferase in *E. coli* and Dr. Anthony Persechini for the MLCK peptide used in this work.

REFERENCES

1. Klee, C. B., Crouch, T. H., and Krinks, M. H. (1979) *Proc. Natl. Acad. Sci. U.S.A.* 76, 6270–6273.
2. Klee, C. B., Guerini, D., Krinks, M. H., De Camilli, P., and Solimena, M. (1990) in *Neurotoxicity of Excitatory Amino Acids* (Guidotti, A., Ed.), Raven Press, New York.
3. Kissinger, C. R., Parge, H. E., Knighton, D. R., Lewis, C. T., Pelletier, L. A., Tempczyk, A., Kalish, V. J., Tucker, K. D., Showalter, R. E., Moomaw, E. W., Gastinel, L. N., Habuka, N., Chen, X., Maldonado, F., Barker, J. E., Bacquet, R., and Villafranca, J. E. (1995) *Nature* 378, 641–644.
4. Hashimoto, Y., Perrino, B. A., and Soderling, T. R. (1990) *J. Biol. Chem.* 265, 1924–1927.
5. Hubbard, M. J., and Klee, C. B. (1989) *Biochemistry* 28, 1868–1874.
6. Griffith, J. P., Kim, J. L., Kim, E. E., Sintchak, M. D., Thomson, J. A., Fitzgibbon, M. J., Fleming, M. A., Caron, P. R., Hsiao, K., and Navia, M. A. (1995) *Cell* 82, 507–522.
7. Klee, C. B., Krinks, M. H., Manalan, A. S., Draetta, G. F., and Newton, D. L. (1985) *Adv. Protein Phosphatases* 1, 135–146.
8. Stemmer, P. M., and Klee, C. B. (1994) *Biochemistry* 33, 6859–6866.
9. Liu, J., Farmer, J. D., Lane, W. S., Friedman, J., Weissman, I., and Schreiber, S. L. (1991) *Cell* 66, 807–815.
10. Clipstone, N. A., Fiorentino, D. F., and Crabtree, G. R. (1994) *J. Biol. Chem.* 269, 26431–26437.
11. Milan, D., Griffith, J., Su, M., Price, E. R., and McKeon, F. (1994) *Cell* 79, 437–447.

12. Perrino, B. A., Fong, Y.-L., Brickey, D. A., Saitoh, Y., Ushio, Y., Fukunaga, K., Miyamoto, E., and Soderling, T. R. (1992) *J. Biol. Chem.* **267**, 15965–15969.
13. Manalan, A. S., and Klee, C. B. (1983) *Proc. Natl. Acad. Sci. U.S.A.* **80**, 4291–4295.
14. Haddy, A., Swanson, S. K.-H., Born, T. L., and Rusnak, F. (1992) *FEBS Lett.* **314**, 37–40.
15. Edsall, J. T. (1958) in *Biophysical Chemistry* (Edsall, J. T., and Wymann, J., Eds.) Vol. 1, pp 591–662, Academic Press Inc., New York.
16. Blumenthal, D. K., and Stull, J. T. (1980) *Biochemistry* **19**, 5608–5614.
17. Huang, C. Y., Chau, V., Chock, P. B., Wang, J. H., and Sharma, R. K. (1981) *Proc. Natl. Acad. Sci. U.S.A.* **78**, 871–874.
18. Blumenthal, D. K., Takio, K., Edelman, A. M., Charbonneau, H., Titani, K., Walsh, K. A., and Krebs, E. G. (1985) *Proc. Natl. Acad. Sci. U.S.A.* **82**, 3187–3191.
19. Anglister, J., Grzesiek, S., Wang, n. C., Ren, H., Klee, C. B., and Bax, A. (1994) *Biochemistry* **33**, 3540–3547.
20. Mondragon, A., Griffith, E. C., Sun, L., Xiong, F., Armstrong, C., and Liu, J. O. (1997) *Biochemistry* **36**, 4934–4942.
21. Duronio, R. J., Jackson-Machelski, E., Heuckeroth, R. O., Olins, P. O., Devine, C. S., Yonemoto, W., Slice, L. W., Taylor, S. S., and Gordon, J. I. (1990) *Proc. Natl. Acad. Sci. U.S.A.* **87**, 1506–1510.
22. Colowick, S. P., and Womack, F. C. (1969) *J. Biol. Chem.* **244**, 774–777.
23. Feldman, K. (1978) *Anal. Biochem.* **88**, 225–235.
24. Hubbard, M. J., and Klee, C. B. (1991) in *Molecular Neurobiology, A Practical Approach* (Chad, J., and Wheal, H., Eds.) pp 135–157, IRL Press, Oxford.
25. Blumenthal, D. K., Takio, K., Hansen, R. S., and Krebs, E. G. (1986) *J. Biol. Chem.* **261**, 8140–8145.
26. Persechini, A., White, H. D., and Gansz, K. J. (1996) *J. Biol. Chem.* **271**, 62–67.
27. Haiech, J., Vallet, B., Robert, A., and Demaille, J. G. (1980) *Anal. Biochem.* **105**, 18–23.
28. Maune, J. F., Klee, C. B., and Beckingham, K. (1992) *J. Biol. Chem.* **267**, 5286–5295.
29. Gill, S. G., and von Hippel, P. H. (1989) *Anal. Biochem.* **182**, 319–326.
30. Sekharudu, Y. C., and Sundralingam, M. (1988) *Protein Eng.* **2**, 139–146.
31. Wei, Q., Xiao, F., Lu, J., and Zhou, J. (1995) *Sci. China B* **38**, 1117–1122.

BI990492W